Slovak University of Technology in Bratislava
Faculty of Civil Engineering

Ing. Svetlana Krišková

Dissertation Thesis Abstract

Numerical modeling of problems of advection on graphs

to obtain the Academic Title of *Philosophiae Doctor (PhD.)*
in the doctorate degree study programme
9.1.9 Applied Mathematics
full-time study

Bratislava 2026

The dissertation thesis has been prepared at the Department of Mathematics and Descriptive Geometry, Faculty of Civil Engineering, Slovak University of Technology in Bratislava

Submitter: Ing. Svetlana Krišková
Department of Mathematics and
Descriptive Geometry
Faculty of Civil Engineering, STU, Bratislava

Supervisor: doc. RNDr. Peter Frolkovič, PhD.
Department of Mathematics and
Descriptive Geometry
Faculty of Civil Engineering, STU, Bratislava

Dissertation Thesis Abstract was sent: .....

Dissertation Thesis Defence will be held on ..... at ..... am/pm at the Department of Mathematics and Descriptive Geometry, Faculty of Civil Engineering, Slovak University of Technology in Bratislava, Radlinského 11, 810 05 Bratislava

prof. Ing. Stanislav Unčík, PhD.
Dean of Faculty of Civil Engineering

Abstract

In the center of the interest of this thesis is the non-conservative advection equation. This hyperbolic partial differential equation serves as a fundamental model for flux propagation in pipe networks. Numerous numerical methods have been developed for problems of this type; however, achieving high accuracy typically requires sufficiently small time steps due to the stability restrictions imposed on commonly used explicit schemes. The method presented in this work aims to overcome these limitations by allowing the use of larger time steps while maintaining stability.

Following [3], the network is modeled as a directed acyclic graph composed of vertices and edges. Within this framework, we derive the so-called inverse WENO scheme, which is conservative in a nonstandard sense, unconditionally stable, without unphysical oscillations even for large Courant numbers, and capable of achieving third order accuracy in both time and space under suitable conditions.

The proposed inverse scheme is tested on various types of networks in a series of numerical experiments. The principal experiment is carried out on a section of the actual sewer network of the city of Revúca, demonstrating the applicability and robustness of the developed method in realistic settings.

Abstrakt

Nosnou témou tejto dizertačnej práce je rovnica advekcie v nekonzervatívnom tvare používana pri modelovaní toku v potrubných systémoch. Pre tento typ úloh je vyvinutých veľké množstvo numerických metód, avšak na dosiahnutie vysokej presnosti a stability, vo veľa prípadoch, je kladená podmienka na dostatočne malé časové kroky pre bežne používané explicitné schémy. Metóda prezentovaná v tejto práci tieto obmedzenia prekonáva tým, že umožňuje použitie väčších časových krokov pri zachovaní stability.

V súlade s [3] je sieť modelovaná ako orientovaný acyklický graf pozostávajúci z vrcholov a hrán. Na pozadí takého to grafu odvodzujeme takzvanú inverznú WENO schému, ktorá je konzervatívna v neštandardnom zmysle, bezpodmienečne stabilná, bez nefyzikálnych oscilácií aj pre veľké Courantove čísla a za vhodných podmienok schopná dosiahnuť presnosť tretieho rádu v čase aj priestore.

Navrhnutá inverzná schéma je aplikovaná na rôzne typy sietí v sérii uvedených numerických experimentov. Hlavný experiment je realizovaný na časti reálnej kanalizačnej siete mesta Revúca, čím sa ukazuje použiteľnosť a všestranosť vyvinutej metódy v realistických podmienkach.

Contents

1 Introduction

Computational and numerical simulations play an essential role in the analysis of many practical applications when the underlying mathematical models are described by partial differential equations (PDEs). A crucial challenge with PDEs is that analytical (exact) solutions are known for only a limited number of simplified equations. To overcome this limitation, numerical methods have been developed to provide accurate approximate solutions.

This thesis focuses partially on fluid dynamics, for which several PDEs of mainly hyperbolic type describe the behavior of fluids at different levels of detail. In the thesis, the hyperbolic equations in their simplest version, the one-dimensional linear advection equation, is treated in details where the main difficulty is their application on networks.

In general, there are two different approaches on how to solve hyperbolic PDEs. The explicit numerical schemes compute solution directly at each time step. They are straightforward in the implementation but require careful selection of the time step size to satisfy stability conditions.

On the other hand, there are so called implicit numerical methods. These methods overcome obstacles with stability, and they are very robust, but it is traded for lower accuracy and slow

convergence of solution. Implicit methods are more demanding both in terms of implementation and computational resources.

We intend to combine the advantages of both approaches. Starting from a Taylor expansion, we apply the inverse Lax–Wendroff procedure to replace spatial derivatives while retaining the time derivatives. This process results in a so-called compact implicit scheme.

However, this scheme may still suffer from the occurrence of non-physical oscillations. To improve the robustness of the compact inverse scheme, we employ Essentially Non-Oscillatory (ENO) and Weighted Essentially Non-Oscillatory (WENO) approximations.

The structure of the thesis is as follows.In the second section, we present the necessary mathematical background for the simulations. It includes a description of the network, which is represented as an acyclic graph.

The third section focuses on the implementation of the proposed numerical methods in the Python programming language.

The fourth section presents fundamental numerical methods required for the derivation of the comapact inverse scheme.

The fifth section focuses specifically on the derivation of the compact inverse scheme. This section also introduces the ENO and WENO schemes, which enhance the method by reducing non-physical oscillations.

The sixth section contains the practical part of the thesis, where several numerical experiments are performed using the schemes derived in the previous sections. First, the methods are tested on a single edge to examine the occurrence of nonphysical oscillations for solutions defined by piecewise functions. Next, the results are compared on a simple network adapted from the [3]. Finally, more complex experiments are performed on a realistic network representing a part of a sewer system

2 Mathematical model

In the beginning, we introduce the notation for networks that can represent in practice sewer systems [7, 1, 10] or district heating networks [2, 8, 3]. We present their formal mathematical description, which can help us introduce the numerical methods and data structures used in their implementation.

Following [5], we suppose that the network is represented by a directed acyclic graph given by a set $\mathcal{V}$ of vertices where $p_m \in \mathcal{V}$, $m = 1, 2, \ldots, M$ and a set $\mathcal{E}$ of oriented edges with two vertices, where $l^e \in \mathcal{E}$, $e = 1, 2, \ldots, E$.

The structure of the network is illustrated in Figure 1.

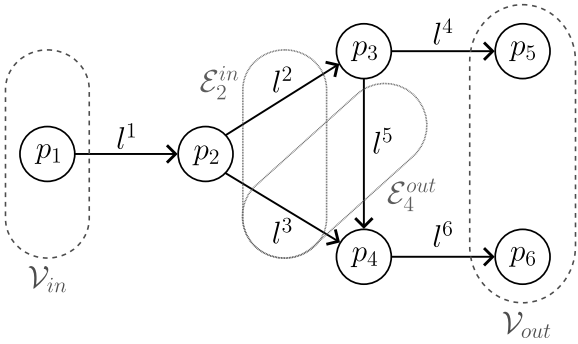

Figure 1: Schematic diagram of the network using the notation outlined in this section.

Now we are ready to formulate the model equation to be

solved on the network in the following form,

$$\partial_t q^e + v^e(t)\partial_x q^e = 0\,, \quad x \in (0, L^e)\,,\ t > 0\,, \quad e = 1, \ldots, E\,.$$

Here, $q^e = q^e(x,t)$, $e = 1, 2, \ldots, E$ is the unknown function related to the edge l^e, where $t \in [0,T] \subset R$ is the time variable and $x \in [0, L^e]$ is the local space coordinate of the edge. The flow rates given $v^e > 0$ can be variable with respect to time. In such a way, q^e can represent the concentration of a transported quantity in the network, e.g. the mass per unit volume [6].

For our purposes, we suppose an initial condition

$$q_0^e(x) = q^e(x,0) = 0\,, \quad x \in (0, L^e)\,, \quad e = 1, 2, \ldots, E\,,$$

In the beginning, there is no transported quantity present in the network.

For the vertices that are not inflow or outflow vertices, we assume the continuity of the concentration.

Our ultimate goal is to apply the proposed method to real-life examples of networks, such as the example of a sewer network in the Slovak city Revúca, see Figure 2.

3 Graphs implementation in Python

The mathematical model presented in section 2 has been implemented using the Python programming language. Python pro-

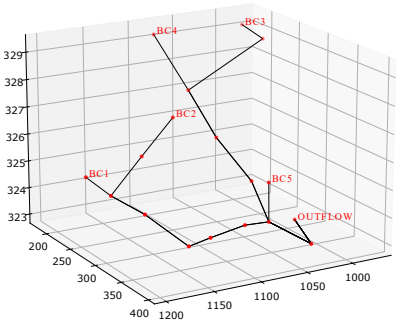

Figure 2: Three dimensional representation of a part of the sewer network in Revúca.

vides a wide range of built-in libraries that support both the specific requirements of this work and the general implementation of numerical methods. In particular, the `NumPy` library is highly suitable for this purpose.

We illustrate the implementation in a specific showcase network, as shown in Figure 1. This network includes multiple vertices and branches that capture the essential elements of the implementation.

The vector `Q` defined as

```
Q = [np.zeros([N + 1, i + 1]) for i in I]
```

is a multidimensional array that will store the approximate values of the computed solution $q_i^n \approx q(x_i, t^n)$ for each edge. It will be calculated at each spatial point x_i^e of every edge $l^e \in \mathcal{E}_m^{in}$ and for each time value t^n. Each dimension of it has a specific meaning.

The first dimension of the array corresponds to the number of edges of the graph for which the results are computed. The second dimension represents the number of discrete time steps and has the same length for all edges. The third dimension corresponds to spatial discretization along each edge and may vary in size depending on the edge.

We introduce a one-dimensional array called `BC` that describes the boundary condition in the following code statement

```
BC = ['BB_b(tt*tau)','alfa[0]*Q[0][tt][I[0]]',
'(1-alfa[0])*Q[0][tt][I[0]]','alfa[1]*Q[1][tt][I[1]]',
'(1-alfa[1])*Q[1][tt][I[1]]',
'Q[2][tt][I[2]]+Q[4][tt][I[4]]'].
```

First, we identify which points serve as vertices. Second, we assign boundary conditions that include information about which edges are connected. Third, this `BC` array also contains data on how the flux is distributed among the branches of our directed graph. In the implementation, we also define the parameter `alpha` as a splitting factor for each splitting vertex

The initial conditions are stored in the `IC` array. For the first edge, whose inlet vertex we define the trigonometric function. The initial condition for this particular showcase is nonzero only on edge 1.

We define `BC` and `IC` as a data type `string` because we need to specify the conditions consisting of the solution itself before

computing the solution. The prescribed code is stored in a `string` array, which allows us to avoid evaluating the boundary condition directly at the place of its establishment.

4 Numerical methods

We focus on a numerical solution of the problems considered. For the derivation of numerical schemes in our work, we begin with the description of the advection equation on a single edge l^e of the network, therefore, we skip the index e in the notation to simplify it,

$$\partial_t q + v(t)\partial_x q = 0\,,\ x \in (0, L)\,,\ t > 0\,. \tag{1}$$

We search for the solution $q = q(x, t)$ of (1) with the boundary and initial conditions given by

$$q(0, t) = q_0(t)\,,\ t \geq 0\,, \quad q(x, 0) = 0\,,\ x \in (0, L)\,.$$

Note that the given velocity function v in (1) is positive, i.e., $v(t) > 0$, $t \geq 0$.

For the space discretization, we will use a notation widely used for the Finite Difference Method (FDM) as it is in [6].

We are looking for approximations $Q_i^n \approx q_i^n$ for $i = 1, 2, \ldots, I$ and $n = 1, 2, \ldots, N$, where $q_i^n := q(x_i, t^n)$ is the exact unknown solution and Q_i^n is an approximate numerical solution using the initial condition $Q_i^0 = 0$ and the boundary condition $Q_0^n = q_0(t^n)$.

4.1 First order implicit method

To overcome this disadvantage of explicit scheme, onr can use implit scheme instead. In the process of obtaining the simplest first order accurate implicit scheme for $v^n > 0$, we aim to approximate the advection equation (1) in the **new time** level $n+1$, i.e., $\partial_t q_i^{n+1} + v^{n+1}\partial_x q_i^{n+1} = 0$. To do so, we again apply the backward finite differences for spatial upwind discretization and for the time discretization (the "backward Euler method") and we obtain the first order implicit scheme :

$$(1 + C_i^{n+1})Q_i^{n+1} - C_i^{n+1}Q_{i-1}^{n+1} = Q_i^n.$$

The implicit schemes generally lead to systems of algebraic equations. The first order accurate methods are inapplicable in practical examples due to their low accuracy.

4.2 Second order explicit method

Considering the stability limitations of fully explicit methods, our aim is to enhance their accuracy. In pursuit of this goal, we focus here on the second order explicit method. The derivation of such a method involves a method known as the **Lax-Wendroff procedure**, also known as **the Cauchy-Kowalewskaya** procedure [6] , where the time derivatives are substituted with spatial derivatives. The procedure will use the advection equation (1). Here, we present only the final form of the second order explicit

scheme, assuming a uniform grid $h_i = h_{i-1}$. The Courant number $C_i^n = C_{i-1}^n \equiv C$ is constant across the spatial domain for a given time step within a single edge. In this case, the stencil can be simplified and implemented in the following form:

$$Q_i^{n+1} = Q_i^n \Big(1 - \frac{3}{2} C w_i + \frac{1}{2} \tau v^n\Big) + Q_{i-1}^n C \Big(\frac{1}{2} + \frac{3}{2} w_i - \tau v^n\Big) + \\ + \frac{1}{2} Q_{i-2}^n C^n \Big(\tau v^n - w_i\Big) - \frac{1}{2} Q_{i+1}^n C (1 - w_i).$$

It is important to mention that the second order explicit scheme is only conditionally stable and in the case of a non-smooth solution, the method could provide numerical results with non-physical oscillations.

5 Inverse scheme

The main contribution of the thesis belongs to this chapter. In order to derive the numerical scheme to solve (1), we begin with the Taylor expansion at point (x_{i-1}, t^n). Next, we apply the inverse Lax-Wendroff procedure to replace the spatial derivatives with the time derivatives, in contrast to the standard Lax-Wendroff method.

To derive the numerical scheme, we use the following parametric finite difference approximations. Firstly, we approximate

$\partial_t q$ by the second order accurate finite differences,

$$\partial_t q_i^n \approx \frac{Q_i^n - Q_i^{n-1}}{\tau} + \frac{1-w}{2\,\tau}\left(Q_i^{n+1} - 2Q_i^n + Q_i^{n-1}\right) + \frac{w}{2\,\tau}\left(Q_i^n - 2Q_i^{n-1} + Q_i^{n-2}\right), \tag{2}$$

and $\partial_{xt} q$ by the first order accurate finite difference,

$$\partial_{xt} q_i^n \approx \frac{1-w}{\tau h}\left(Q_i^{n+1} - Q_i^n - Q_{i-1}^{n+1} + Q_{i-1}^n\right) + \frac{w}{\tau h}\left(Q_i^n - Q_{i-1}^n - Q_i^{n-1} + Q_{i-1}^{n-1}\right), \tag{3}$$

The final parametric numerical scheme for a single edge l^e and for $C_i^n > 0$ in the network takes the form

$$\begin{aligned} C_i^n Q_i^n + Q_i^n - \frac{1}{2}\big((1-w^n)(Q_{i-1}^{n+1} - Q_i^n) + \\ + w^n(Q_{i-1}^n - Q_i^{n-1})\big) = \\ C_i^n Q_{i-1}^n + Q_i^{n-1} - \frac{1}{2}\big((1-w^{n-1})(Q_{i-1}^n - Q_i^{n-1}) + \\ + w^{n-1}(Q_{i-1}^{n-1} - Q_i^{n-2})\big), \end{aligned} \tag{4}$$

where we emphasize that w can be time dependent. We assume that the values Q_i^0 and Q_i^1 for $i = 0, 1, \ldots, I$ and also Q_0^n for $n = 2, 3, \ldots, N$ are given.

The scheme is **unconditionally stable** using von Neumann stability analysis for constant (or frozen) velocity values as shown in [4] for the case of a direct numerical scheme.

We describe how to choose the values w^n of the parameter. If the velocity is constant in time, i.e., the Courant number is

constant and $C^n = C^{e,n} \equiv C^e$, then the best choice based on our previous research published in [4] is

$$w^n = \frac{1}{3} + \frac{1}{6C^{e,n}}\,. \tag{5}$$

In this setting of the parameter w^n, the scheme (4) achieves third order accuracy in both time and space. In general, for non-smooth, discontinuous, or rapidly varying solutions, the numerical scheme (4) might produce unphysical oscillations.

To make the scheme (4) able to solve such cases as those with discontinuous solution and suppress non-physical oscillations, we introduce a modified form of the parameter w^n, making it dependent on the numerical solution itself, i.e., $w^n = w(Q_i^n)$. This brings nonlinearity but this difficulty can be handled using a predictor-corrector iterative approach.

One of the simplest ways to avoid unphysical oscillations is to use the **Essentially Non-Oscillatory** (ENO) scheme. The ENO scheme adaptively selects its stencil. Near discontinuities, the stencil selection process chooses grid points exclusively from one side of the discontinuity.

Note that although ENO introduces nonlinearity into the computation process as the decision on the final stencil depends on the solution itself thanks to the parameter $w(r)$, it will be relaxed by the predicted value $Q_i^{n,p}$.

In our work, we also improved the compact inverse scheme (4)

with the **Weighted Essentially Non-Oscillatory (WENO)** scheme. The WENO is an extension of the ENO. The difference lies in how the stencils are chosen, WENO retains all candidate stencils, evaluates their smoothness, and assigns each a weight based on its.

In regions where there is a presence of discontinuities and the scheme generates non-physical oscillations, an indicator penalizes stencils that cross the discontinuity, assigning them very small weights, while simultaneously giving greater weight to the more suitable, smooth stencils.

We consider the weights as polynomial-based functions. In this work, both theoretical formulation and numerical experiments employ indicators based on second-degree polynomials.

So finally the WENO wights reach the form :

$$w = \frac{2\Big(\epsilon + (Q_i^{n+1} - Q_i^n)^2\Big)^2}{\Big(\epsilon + (Q_i^{n+1} - Q_i^n)^2\Big)^2 + 2\Big(\epsilon + (Q_i^{n+1} - Q_i^n)^2\Big)^2}$$

6 Numerical experiments

We would like to demonstrate the behavior of compact implicit inverese scheme (4) and compare its propherties, in the case of variable parameter w (WENO) with the fixed value of w (3rd order inverse scheme). We performed experiments on the single

edge and also on networks. In each case, we compare **the experimental order of convergence (EOC)** for each numerical method.

6.1 Benchmark with a non-smooth solution

We start testing our schemes for a single edge with non-smooth solution for the occurrence of nonphysical oscillations. We evaluate the influence of the doubled number of time steps $\tau = 0.005$ on the precision and presence of nonphysical oscillation, see Figure 3. The 3rd order inverse scheme provides values closer to the values of exact solution but suffers from presence of non-psysical oscillation. The lower value of the Cournat number increases the precision of the numerical solution for both presented schemes and WENO schemes that successfully suppress oscillations.

6.2 Numerical experiments on a realistic network

We apply our numerical schemes to a part of a real sewer network in the city of Revúca. The final form of the network with which we are working is plotted in Figures 4 and 2. We note that in the current version we derive a nondimensional model based on this network to assess the behavior of our numerical method for some possible scenarios of pollutant transport [9] in complex networks.

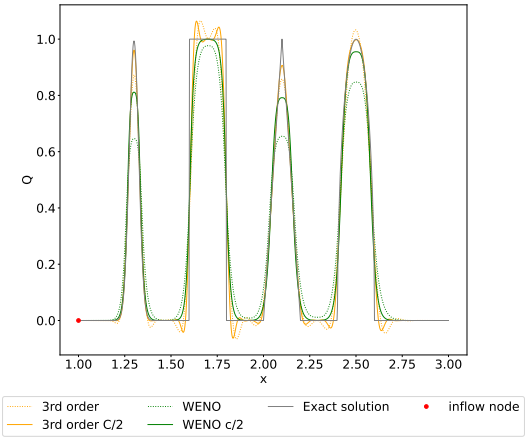

Figure 3: Comparison of methods in addtion to change of Cournat number. Dotted line for $C = 4.$ and simple line for $C/2 = 2.$

The network consists of five input vertices and one output vertex denoted by `OUTFLOW` see Figure 4.

6.2.1 Constant water discharge

In our experiment, we suppose constant velocities per each edge to represent a stationary flow in the network. The values are obtained by prescribing constant water discharge (volume flow) V_{bc} for each input vertex.

For our numerical experiment in this network, we set the final simulation time $T = 2$. The number of time steps gradually $N = 192,384$. The number of spatial steps I^e per each edge l^e is

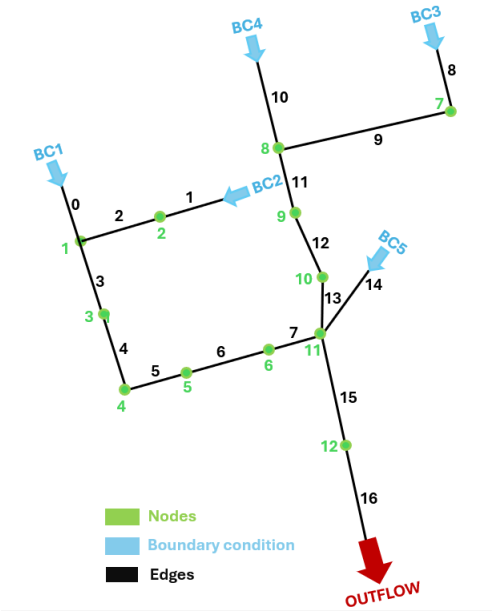

Figure 4: 2D representation of the part of the sewer Revuca

128 or 256 to take into account the significantly different lengths of the edges in the network. The Courant numbers C^e for each edge are shown in Tables 1, 2.

e	0	1	2	3	4	5	6	7	8
I^e	96	96	96	96	96	96	96	96	96
C^e	5.23	2.33	2.42	7.40	7.17	4.75	3.39	5.12	16.03

e	9	10	11	12	13	14	15	16	
I^e	192	96	96	96	96	96	192	192	
C^e	1.76	4.25	10.74	10.36	12.03	4.84	7.04	4.30	

Table 1: Courant numbers for edges, N = 192.

e	0	1	2	3	4	5	6	7	8
I^e	96	96	96	96	96	96	96	96	96
C^e	2.61	1.16	1.21	3.70	3.58	2.37	1.69	2.56	8.015

e	9	10	11	12	13	14	15	16	
I^e	192	96	96	96	96	96	192	192	
C^e	0.88	2.12	5.37	5.18	6.01	2.42	3.52	2.15	

Table 2: Courant numbers for edges, N = 384.

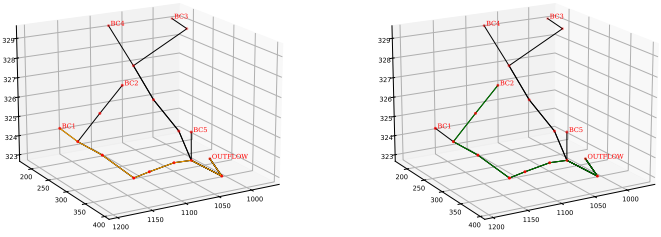

(a) Path BC1 (b) Path BC2

Figure 5: Selected paths of the Revúca sewer network.

To demonstrate the results, we mark paths originating from the inflow vertices $BC1 - BC5$, respectively, as shown in Figures 5, each path terminating at the `OUTFLOW` vertex. In all cases, clearly, the waves are moving towards the `OUTFLOW` vertex. The flow profile along selected paths at different times is shown in the series of Figures 5a, 5b. We mark the coupling vertices with dashed lines in these Figures together with the vertex number. Note that we should observe in the solution the waves of the prescribed initial maximal value that are eventually summed up and that can change their lengths due to different speeds on each edge. In Figures, we present the numerical solutions obtained with the 3rd order accurate scheme (4) with (5).

Figure 6 shows the path that starts at $BC1$. We could notice

that the shape of the wave is changing over time.

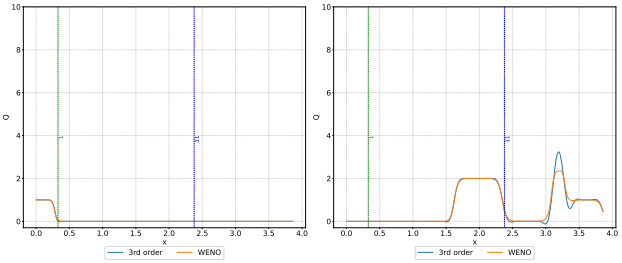

(a) t = 0.25 (b) t = 2.0

Figure 6: Flow through the path $BC1$ shown in 2 different moments. Courant numbers on each edge are shown in Table 2.

For $t = 2$ one can observe interactions of the waves. At $t = 2$, the waves that originated from $BC1, BC3$ and $BC2$ are in the system, where the undershooting $Q_{max} \approx 2.39$ for the WENO scheme is clearly visible, as well as overshooting in the case of *the 3rd order accurate scheme* $Q_{max} \approx 3.24$. The maximum value of this wave is set to 3 in the boundary condition.

We also observe that the impact of the doubled number of time steps is presented in Table 1 and Table 2. The series of Figures 7 describes the path $BC2$ in the final time $t = 2$ where the accuracy of the results offered by the 3rd order and WENO schemes could be visually compared.

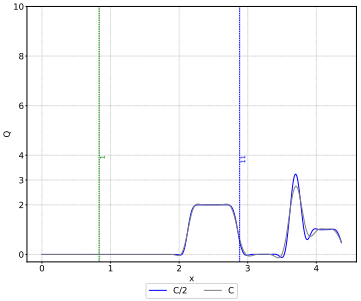

(a) 3rd order

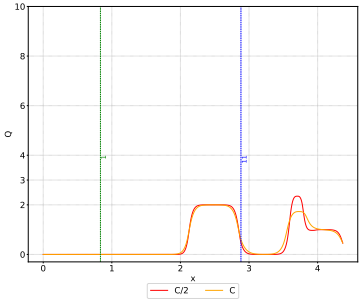

(b) WENO

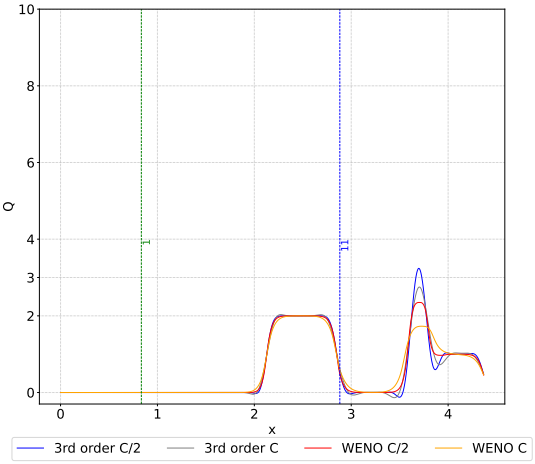

(c) 3rd order & WENO

Figure 7: Flow through the path $BC2$ shown in t = 2. Comparison of inverse schemes with variable w - WENO and fixed w - 3rd order

References

[1] Banik, BK., Di Cristo, C., and Leopardi, A. SWMM5 toolkit development for pollution source identification in sewer systems. *Procedia Eng. 89* (2014), 750–757.

[2] Borsche, R., Eimer, M., and Siedow, N. A local time stepping method for thermal energy transport in district heating networks. *Appl. Math. Comp. 353*, C (2019), 215–229.

[3] Eimer, M., Borsche, R., and Siedow, N. Implicit finite volume method with a posteriori limiting for transport networks. *Adv Comput Math 48*, 3 (2022), 21.

[4] Frolkovič, P., Krišková, S., Rohová, M., and Žeravỳ, M. Semi-implicit methods for advection equations with explicit forms of numerical solution. *Japan Journal of Industrial and Applied Mathematics* (2022), 1–25.

[5] Frolkovič, P., Krišková, S., and Lacková, K. Unconditionally local bounds preserving numerical scheme based on inverse Lax–Wendroff procedure for advection on networks. *Computers & Fluids 301* (Oct. 2025), 106806.

[6] LeVeque, R. J. *Finite volume methods for hyperbolic problems*, vol. 31. Cambridge university press, 2002.

[7] Mark, O., Wennberg, C., van Kalken, T., Rabbi, F., and Albinsson, B. Risk analyses for sewer systems based on numerical modelling and GIS. *Safety Science 30*, 1 (1998), 99–106.

[8] Mohring, J., Linn, D., Eimer, M., Rein, M., and Siedow, N. District heating networks–dynamic simulation and optimal operation. *Math. Model. Simul. Optim. Power Eng. Manag.* (2021), 303–325.

[9] Sokáč, M., and Velísková, Y. Impact of Sediment Layer on Longitudinal Dispersion in Sewer Systems. *Water 13*, 22 (2021), 3168.

[10] Velísková, Y., Sokáč, M., and Moghaddam, M. B. Inverse task of pollution spreading – Localization of source in extensive open channel network structure. *J. Hydrol. Hydromech. 71*, 4 (2023), 475–485.

List of author's publications

- FROLKOVIČ, Peter - KRIŠKOVÁ, Svetlana [Šaušová, Svetlana,] - ROHOVÁ, Michaela - ŽERAVÝ, Michal. Semi-implicit methods for advection equations with explicit forms of numerical solution. In Japan Journal of Industrial and Applied Mathematics. Vol. 39, iss. 3 (2022), s. 843-867. ISSN 0916-7005 (2022: 0.900 - IF, Q3 - JCR Best Q, 0.374 - SJR, Q2 - SJR Best Q). V databáze: SCOPUS: 2-s2.0-85141399134 ; CC: 000890328700003 ; DOI: 10.1007/s13160-022-00525-y.
- FROLKOVIČ, Peter - KRIŠKOVÁ, Svetlana [Šaušová, Svetlana,] - LACKOVÁ, Katarína. Unconditionally local bounds preserving numerical scheme based on inverse Lax–Wendroff procedure for advection on networks. In Computers & Fluids. No. 301 (2025), [16] s., art. no. 106806. ISSN 0045-7930 (2024: 3 - JIF, Q2 - JIF Best Q, 0.878 - SJR, Q1 - SJR Best Q, 0.772 - AIS, Q1 - AIS Best Q). V databáze: SCOPUS: 2-s2.0-105014739279 ; DOI: 10.1016/j.compfluid.2025.106806 ; CC: 001565126700001.